

Weakly Supervised Semantic Segmentation via Alternative Self-Dual Teaching

Dingwen Zhang¹, Wenyuan Zeng¹, Guangyu Guo¹, Chaowei Fang², Lechao Cheng³, Junwei Han¹

¹The Brain and Artificial Intelligence Laboratory, Northwestern Polytechnical University, Xi'an, China

²Xidian University, Xi'an, China

³Zhejiang Lab, Hangzhou, China

¹https://nwpu-brainlab.gitee.io/index_en

Abstract

Current weakly supervised semantic segmentation (WSSS) frameworks usually contain the separated mask-refinement model and the main semantic region mining model. These approaches would contain redundant feature extraction backbones and biased learning objectives, making them computational complex yet sub-optimal to addressing the WSSS task. To solve this problem, this paper establishes a compact learning framework that embeds the classification and mask-refinement components into a unified deep model. With the shared feature extraction backbone, our model is able to facilitate knowledge sharing between the two components while preserving a low computational complexity. To encourage high-quality knowledge interaction, we propose a novel alternative self-dual teaching (ASDT) mechanism. Unlike the conventional distillation strategy, the knowledge of the two teacher branches in our model is alternatively distilled to the student branch by a Pulse Width Modulation (PWM), which generates PW wave-like selection signal to guide the knowledge distillation process. In this way, the student branch can help prevent the model from falling into local minimum solutions caused by the imperfect knowledge provided of either teacher branch. Comprehensive experiments on the PASCAL VOC 2012 and COCO-Stuff 10K demonstrate the effectiveness of the proposed alternative self-dual teaching mechanism as well as the new state-of-the-art performance of our approach.

1. Introduction

Semantic segmentation is a widely studied problem in computer vision. Traditional semantic segmentation approaches, such as [49, 69], train their models under the fully supervised learning manner, where the pixel-wise manual annotation is required to facilitate the learning process. However, pixel-wise manual annotation tends to be much more difficult to acquire due to its high human labor and time costs. In order to realize the learning process of semantic

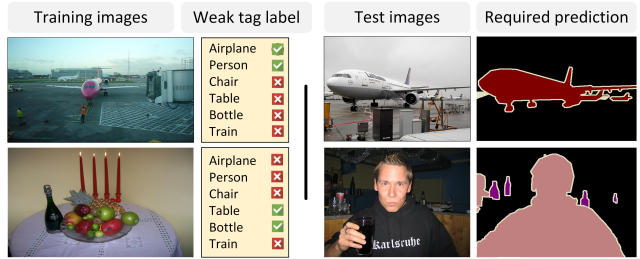


Figure 1. Brief illustration of the investigated weakly supervised semantic segmentation task.

segmentation model with less annotation cost, a recent trend in this research field is to develop weakly supervised semantic segmentation (WSSS) frameworks, under which the learning process won't require the pixel-wise manual annotation anymore. Instead, the annotation might be short scribbles [46, 64, 65, 68], bounding boxes [12, 52], points [5, 50], or image tags [27, 40], and this paper focuses on the last learning scenario (see Fig. 1).

In WSSS, the key problem is how to generate the pixel-wise pseudo segmentation masks for training images. One fundamental solution to this problem is to adopt the class-activation mapping-based classification model [84] in the training phase, where the intermediate deep feature maps that correspond to certain semantic classes can be used to generate the pseudo segmentation masks. To avoid learning feature maps that only focus on the discriminative but incomplete object regions, a series of follow-up works, such as [8, 15, 62, 71, 78], proposed carefully designed variants of the class-activation mapping mechanism and obtained the desired performance gains. However, as the pseudo segmentation masks generated by these methods are still from the intermediate feature maps, they inevitably have ununiform responses on object regions and inadequate object boundary details.

For addressing this limitation, some current WSSS models are devised by employing the class-activation mapping (or its variations)-based classification model first to obtain

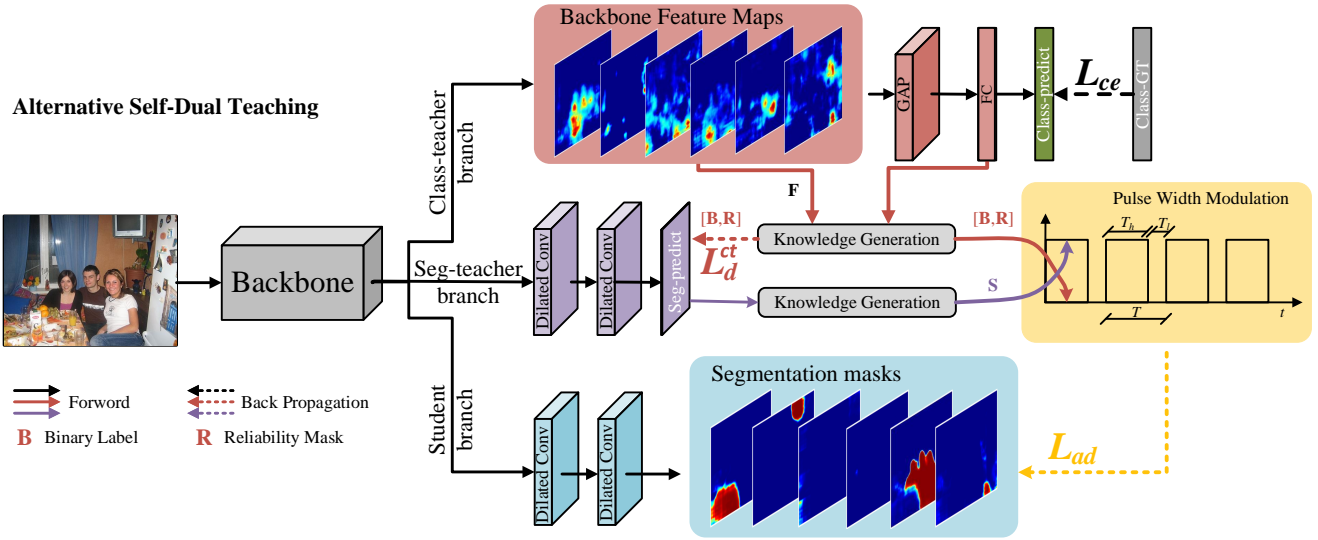


Figure 2. The overall framework of the proposed weakly supervised semantic segmentation approach.

the discriminative semantic seeds followed by other post-processing strategies, e.g., [30, 76], or learning-based refinement model, e.g., [9, 14, 34, 81], to generate more acceptable segmentation masks as the pseudo label. However, due to the insufficient knowledge sharing and interaction, the models used in such methods usually contain redundant feature extraction backbones, biased learning objectives, and may also rely on external prior knowledge such as objectness [3] and saliency [20]. All these make them computational complex yet solution sub-optimal.

To this end, Zhang *et al.* [77] proposed the first unified deep weakly supervised learning model to obtain the high-quality pseudo segmentation masks. They implement a classification branch and a refinement branch via a shared feature extraction backbone. This design can facilitate knowledge sharing between the two components at the feature level and make the whole learning framework have low computational complexity. To produce the self-guidance to learn the refinement component, i.e., the segmentation branch, Zhang *et al.* [77] propose to mine the confident semantic regions from the classification branch and use them as the supervision signals of the segmentation branch. Such a learning framework can actually be interpreted as a teacher-student model with a straightforward knowledge distillation path, capable of propagating knowledge from the teacher branch to the student branch. Due to the label smoothing effect [82], knowledge distillation has been demonstrated to be an effective way to improve the performance of the student model in different scenarios [4, 18, 23]. It may also explain the impressive experimental results obtained by [77].

However, unlike distilling knowledge under the fully supervised learning scenarios, the knowledge of the teacher model learned under weak supervision may have very low quality. Under this circumstance, constantly distilling knowl-

edge from the teacher model to the student model would make the student model biased to sub-optimal solutions. Consequently, directly using the conventional straightforward knowledge distillation path in [77] could not maximize the benefit to the student model. More careful designs are urgently needed to implement the knowledge distillation from the teacher to the student model.

To solve this problem, this paper makes an early effort to facilitate a more reliable yet artful knowledge distillation process, called alternative self-dual teaching, to encourage the knowledge interaction between the teacher and student model under weak supervision. It has two-fold novel designs. Firstly, unlike the single-teacher model presented in [77], our ASDT is a dual teacher model, which is equipped with two teacher network branches to improve the diversity of the knowledge for distillation. While a more substantial property is that when performing knowledge distillation to train the student model, we adopt a novel alternative distillation scheme. Compared to the straightforward distillation scheme, our proposed alternative distillation scheme won't constantly distill knowledge from a certain teacher model. Instead, it alternatively distills knowledge from the two teacher branches to the student branch by following the PW wave-like selection signal that is generated by a Pulse Width Modulation. In this way, the knowledge distilled from one teacher branch could help the student branch to get rid of local minimum solutions that would be derived by the other teacher branch, and vice versa. Such an alternative distillation scheme would help the student model converge to a more promising solution as shown in Fig. 4.

This work mainly has three-fold contributions:

- We make an early effort to introduce knowledge distillation to WSSS and establish a self-dual teaching-based unified deep model to generate the high-quality pseudo

segmentation masks.

- We propose a novel alternative distillation scheme to increase the knowledge interaction between the teacher and student networks. It can help avoid the student model getting into the local minimum solutions caused by the imperfect knowledge of either teacher model, thus playing an essential role in the weakly supervised learning scenario.
- Comprehensive experiments on two widely-used benchmarks have been implemented to evaluate the performance of the proposed approach. The experimental results demonstrate that such an easy-to-implement scheme can obtain superior segmentation performance compared to the existing state-of-the-art methods.

2. Related Works

Weakly supervised semantic segmentation: For weakly-supervised semantic segmentation (WSSS), the model is supervised by various types of partial labels, such as bounding boxes [12, 41, 51, 52, 61], scribbles [46, 64, 65, 68], points [5, 50], and image-level class labels [25, 27, 35, 36, 40, 42, 45]. WSSS under image-level supervision is the most challenging among all these categories as they require minimal effort for human annotation. Approaches designed in early ages operate only with the image-level supervision without using additional information [1, 2, 8, 9, 33, 40, 44, 60, 70, 71, 77–79]. Most of these kinds of methods first generate pseudo-labels based on CAMs [84], and then train a supervised semantic segmentation network such as DeepLab-v1 [10], DeepLab-v2 [11]. While many recent approaches introduce extra information into the WSSS training process to obtain better performance [32, 39, 48]. In these methods, saliency map [6] usually works as the most popular prior information as it can provide accurate boundary information [14, 15, 27, 34, 36, 38, 39, 48, 57, 62, 73, 81]. While some other methods introduce extra training images such as noisy images obtained from web [31, 39, 62], YouTube videos [24], or ImageNet (*i.e.* 24K ImageNet) [16, 26, 48]. In this paper, we design a novel WSSS framework only using the image-level supervision.

Knowledge distillation: Knowledge distillation [4, 18, 23] aims to transfer knowledge from a well-trained teacher network to a compact student network. In the classical knowledge distillation approaches, the student networks are supervised by information extracted from the teacher networks, such as predicted probabilities [4, 23], intermediate features [53, 58, 67], *etc.* Differently, the self-distillation mechanism transfers knowledge within a model itself [18, 37, 55, 74, 80]. For example, Zhang *et al.* [80] transferred knowledge from the deeper layers of a neural network into its shallow layers. Phuong *et al.* [55] guided the learning of a current network layer by the output of network

layer behind it. Yang *et al.* [74] utilized the information of earlier training epochs to supervise the later training epochs. The self-distillation mechanism has been applied in many fields like classification [80], weakly-supervised object detection [28], text segmentation [75], *etc.* In this paper, we introduce the self-distillation mechanism into the training process of the WSSS model and propose a novel self-dual teaching strategy to facilitate an effective knowledge distillation under the weak supervision.

3. The Overall Approach

Given training image collection \mathcal{X} and the corresponding image-level label collection \mathcal{Y} , the goal is to learn a deep model to predict pixel-level semantic segmentation map $\bar{\mathbf{P}}$ for a test image \mathbf{X} .

To achieve this goal, we build a unified learning model to embed both the image-level classification and pixel-level expansion components. As shown in Fig. 2, it first has a feature extraction backbone. Then, the proposed deep model is constructed by a self-dual teaching architecture, which contains three parallel network branches including a class-teacher branch $f_{ct}(\cdot)$, a seg-teacher branch $f_{st}(\cdot)$, and a student branch $f_s(\cdot)$. During training, the two teacher network branches distill gainful knowledge, including \mathbf{R}^{ct} , \mathbf{B}^{ct} , \mathbf{P}^s , and \mathbf{B}^{st} (details can be referred to Sec. 3.1), to the student network branch, enabling the student network to learn strong patterns for generating satisfied semantic segmentation masks. To enrich knowledge interaction between the teacher network branches and the student network branch, we further develop an alternative distillation mechanism in comparison to the conventional straightforward knowledge distillation (details can be referred to Sec. 3.2).

After the above-mentioned learning process, we obtain the segmentation prediction for each training image by collaborating the seg-teacher network branch and the student network branch as both of them can predict the pixel-level semantic. Specifically, we first combine the predictions of the seg-teacher network branch \mathbf{P}^{st} and the student network branch \mathbf{P}^s by:

$$\bar{\mathbf{P}} = \Delta \max[\mathbf{P}^{st}, \mathbf{P}^s], \quad (1)$$

where $\Delta \max$ indicates the element-wise maximization operation for the input matrix. As one of the common operation in this research field, we then generate the final segmentation prediction by performing CRF-based post-processing to $\bar{\mathbf{P}}$.

3.1. Self-Dual Teaching Architecture

The proposed self-dual teaching architecture contains two teacher network branches and a student network branch. The first teacher network branch is a class-activation mapping-based classification branch. We treat it as a class-teacher branch $f_{ct}(\cdot)$. In this branch, we first perform the global average pooling (GAP) [84] on the feature maps extracted by the

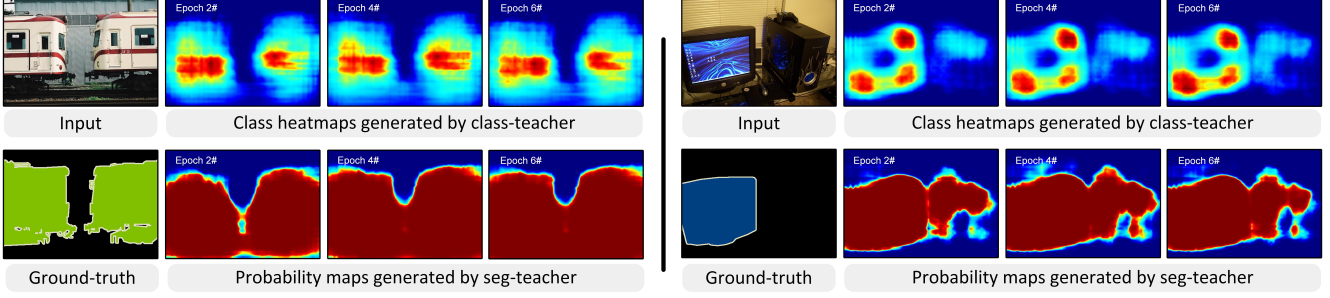


Figure 3. Examples to show different characteristics of the knowledge extracted by the class-teacher branch and seg-teacher branch. As can be seen, the class-teacher would focus on the local parts of the whole objects of interest, while the seg-teacher would segment out more visually similar regions but introduce miss-classification regions.

feature extraction backbone \mathbf{F} . Then, a fully-connected layer is adopted to map the pooled feature vector to the image-level classification prediction. Then, the whole process of this teacher network branch can be denoted as $\hat{\mathbf{y}} = f_{ct}(\mathbf{F}, \mathbf{W}_{ct})$, where \mathbf{W}_{ct} indicates the learnable parameters of this network branch. Under the supervision of the ground-truth image tag annotation $\mathbf{y} = [y_1, y_2, \dots, y_C]$, where C indicates the total number of the explored classes, we can then learn the class-teacher by minimizing:

$$\mathcal{L}_{ce} = - \sum_{c=1}^C [y_c \ln \hat{y}_c + (1 - y_c) \ln(1 - \hat{y}_c)]. \quad (2)$$

For distilling helpful knowledge to guide other network branches, we follow [84] to associate the feature maps \mathbf{F} with the learned weights in the fully-connected layer, thus generating the class-wise heat-maps $\mathcal{H} = \{\mathbf{H}_c\}_{c=1}^C$. It is worth noting that the knowledge encoded in \mathcal{H} is obtained under weak supervision, which always contains inaccurate or incomplete responses. To tackle this issue, we follow [77] to generate the binary label matrix $\mathbf{B}^{ct} \in \mathbb{R}^{h \times w \times (C+1)}$ and the reliability mask $\mathbf{R}^{ct} \in \mathbb{R}^{h \times w}$ based on \mathcal{H} , where the reliability mask \mathbf{R}^{ct} can help screen the sparsely yet highly activated noisy regions produced by the CAM to guide a stable learning procedure. Then, the obtained binary label matrix \mathbf{B}^{ct} and reliability mask \mathbf{R}^{ct} are the knowledge that will be used in the subsequent knowledge distillation process.

The second teacher network branch is a segmentation-oriented branch termed seg-teacher $f_{st}(\cdot)$ with parameters \mathbf{W}_{st} , where we use two 3×3 dilated convolutional layers with the dilation rate as 12 and a softmax operation at the end of the branch. The branch is trained directly under the guidance of the knowledge distilled from the classification branch via a structured distillation loss \mathcal{L}_d^{ct} that will be introduced in the following subsection. Once this teacher network branch is trained, we can use its forward path to generate the $C + 1$ -channel probability maps \mathbf{P}^{st} and then employ the CRF-based post-processing to \mathbf{B}^{st} .

The student network branch $f_s(\cdot)$ has the same architecture as $f_{st}(\cdot)$ but with unshared network parameters \mathbf{W}_s . It

is trained based on the knowledge distilled from the above two teacher branches under the alternative distillation mechanism (see the details in the next subsection) and predicts the $C + 1$ -channel probability maps $\mathbf{P}^s = f_s(\mathbf{F}|\mathbf{W}_s)$.

3.2. Alternative Distillation Mechanism

In the proposed self-dual teaching architecture, the two teacher network branches have different network designs and are learned in different manners—The class-teacher $f_{ct}(\cdot)$ is learned under the image-level weak supervision, while the seg-teacher $f_{st}(\cdot)$ is learned under the self-produced supervision. Under this circumstance, the guidance knowledge generated by the two teacher models would have different properties as well: The class-teacher would overweight the classification results of the image so that it focuses more on the local discriminative object parts but ignores the less discriminative yet indispensable object parts (see top row of Fig. 3). On the contrary, the seg-teacher would overweight the classification results on each pixel localization to pursue high segmentation performance so that it can segment out the large portion of the object regions but would miss-classify the image regions with the large intra-class variation or inter-class similarity (see bottom row of Fig. 3).

From the above discussion, we can see that both of the teacher models have their own merits to distill helpful knowledge but neither of them is perfect. Under this circumstance, directly distilling knowledge from either the class-teacher or the seg-teacher would lead the student network branch to stick into undesired local minimum solution (see Fig. 4). To solve this problem, we propose a novel alternative distillation mechanism. Under this mechanism, the knowledge used to guide the learning process of the student network branch is alternatively distilled from the class-teacher and the seg-teacher with a selection signal generated by a PWM¹ (see Fig. 2). Specifically, the alternative distillation loss is

¹Pulse-width modulation is a widely used technique in signal system, which uses a rectangular pulse wave whose pulse width is modulated resulting in the variation of the surpassing signal https://en.wikipedia.org/wiki/Pulse-width_modulation.

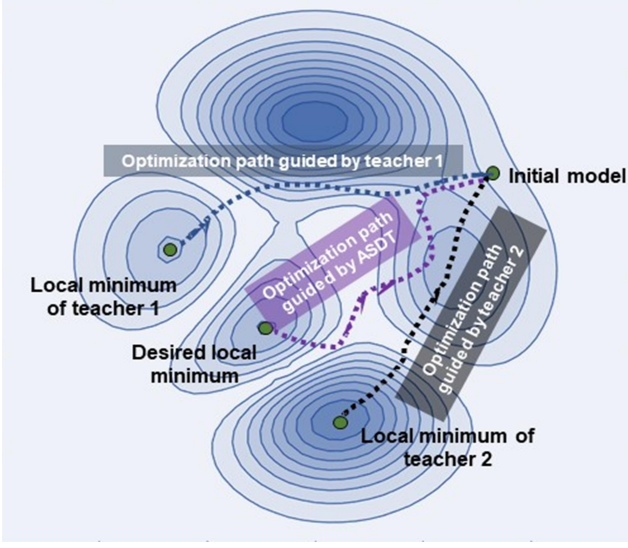


Figure 4. Diagrammatic drawing of the gradient descent trajectory of different learning schemes².

defined as:

$$\mathcal{L}_{ad} = \Lambda_t(\mathcal{L}_d^{ct}(\mathbf{P}^s, [\mathbf{B}^{ct}, \mathbf{R}^{ct}]), \mathcal{L}_d^{st}(\mathbf{P}^s, \mathbf{B}^{st}) | T, \tau), \quad (3)$$

where $\Lambda_t(\cdot)$ is the knowledge selection function for alternatively selecting the guiding knowledge under the PW wave signal at the iteration time t . T and τ are the hyper-parameters for identifying the PW wave signal, where T indicates the alternation period width while τ indicates the proportion of the class-teacher and the seg-teacher, i.e., $\tau = T_l/T_h$. Here T_h and T_l are the length of the high level signal (the signal to select the seg-teacher for knowledge distillation) and the low level signal (the signal to select the class-teacher for knowledge distillation) in one alternation period width, i.e., $T = T_h + T_l$. The PW wave signal can be referred to in Fig. 2.

To assist the knowledge distillation process, we consider the spatial structure and low-level appearance consistency in \mathcal{L}_d^{ct} and \mathcal{L}_d^{st} . Specifically, we define

$$\mathcal{L}_d^{ct} = \sum_i \sum_{c \in \mathcal{C}^+} r_i^{ct} b_{c,i}^{ct} \log(p_{c,i}^s) + \mathcal{L}_{str}, \quad (4)$$

$$\mathcal{L}_d^{st} = \sum_i \sum_{c \in \mathcal{C}^+} b_{c,i}^{st} \log(p_{c,i}^s) + \mathcal{L}_{str}, \quad (5)$$

where r_i^{ct} , $b_{c,i}^{ct}$, $p_{c,i}^s$, $b_{c,i}^{st}$ are the elements in \mathbf{R}^{ct} , \mathbf{B}^{ct} , \mathbf{P}^s , and \mathbf{B}^{st} , respectively.

From the above formulation, we can observe that different from the conventional knowledge distillation methods that use the soft label as the guidance knowledge, we use the hard label instead. This is because the conventional knowledge

²The local minimum would not necessarily indicate the prediction results, it could also be interpreted as the intermediate features of the network.

distillation methods work under the supervised learning scenario, where the teacher models can usually reach a perfect level. According to the Transfer Risk Bound established by [29], a high ratio of teacher’s soft labels can be beneficial under this circumstance. In contrast, the knowledge distillation process performed by our framework is under weak supervision, where the teacher models cannot be perfect. Under this circumstance, using the soft label would introduce more disturbing knowledge that hurts the learning of the student model, while using the hard labels can sometimes correct the teacher’s wrong prediction [29].

In fact, the soft labels that are usually used in the conventional distillation scenarios provide the semantic dependency to benefit the learning of the student model. To make up for its lack, we introduce \mathcal{L}_{str} to guide the distillation process in Eq. 4 and 5, which explores the spatial and low-level appearance dependency instead. Specifically, to encode the spatial structure and low-level appearance consistency, we define

$$G_{i,j} = \frac{1}{Z} \exp \left(-\frac{\|\mathbf{D}_i - \mathbf{D}_j\|^2}{2\sigma_D^2} - \frac{\|\mathbf{I}_i - \mathbf{I}_j\|^2}{2\sigma_I^2} \right) \quad (6)$$

as the Gaussian kernel bandwidth filter, where Z is the normalization factor, \mathbf{D}_i indicates the spatial location of the i -th pixel, while \mathbf{I}_i indicates its RGB color. σ_D and σ_I are the Gaussian kernel parameters. Then, we apply the Potts model [65] to formulate the structure energy as:

$$E_{i,j} = G_{i,j} \sum_{c \in \mathcal{C}^+} p_{c,i}^s (1 - p_{c,j}^s). \quad (7)$$

Considering that such structure energy would play a more important role in guiding the learning of the less confident pixels, i.e., those with the smaller predicted probability values, we define the structure loss as:

$$\mathcal{L}_{str} = \sum_i \sum_{j \neq i} (1 - \max_{c \in \mathcal{C}^+} p_{c,i}^s) E_{i,j}. \quad (8)$$

Since the spatial and low-level appearance dependency could provide more confident knowledge than the semantic dependency under the investigate weakly supervised learning scenario, the proposed learning framework can facilitate an effective learning procedure.

4. Experiments

Dataset and Evaluation Metric. Experiments are conducted on the Pascal VOC 2012 [13] dataset and COCO-Stuff 10K [47]. On the Pascal VOC 2012, following the

³<http://host.robots.ox.ac.uk:8080/anonymous/HMPFSZ.html>

⁴<http://host.robots.ox.ac.uk:8080/anonymous/R9XFGZ.html>

Table 1. Comparison with the state-of-the-art approaches on PASCAL VOC 2012 *val* and *test* sets. the supervision information (Sup.) includes: F (full pixel-level supervision), I (image-level supervision), B (bounding box-level supervision), S (scribble-level supervision), SA (saliency maps).

Method	Pub.	Backbone	Sup.	val	test
DeepLab-v1 [10]	ICLR15	VGG-16	F	67.6	70.3
Deeplab-v2 [11]	PAMI17	ResNet-101	F	76.8	79.7
WSSL [52]	ICCV15	VGG-16	B	60.6	62.2
BBAM [41]	CVPR21	ResNet-101	B	73.7	73.7
Oh <i>et al.</i> [41]	CVPR21	ResNet-101	B	74.6	76.1
KernelCut [65]	ECCV18	ResNet-101	S	75.0	-
BPG [68]	IJCAI19	ResNet-101	S	76.0	-
Fan <i>et al.</i> [15]	ECCV20	ResNet-101	I, SA	67.2	66.7
Lee <i>et al.</i> [39]	ICCV19	ResNet-101	I, SA	66.5	67.4
MCIS <i>et al.</i> [62]	ECCV20	ResNet-101	I, SA	67.7	67.5
ICD [14]	CVPR20	ResNet-101	I, SA	67.8	68.0
LIID [48]	PAMI20	ResNet-101	I, SA	67.8	68.3
Li <i>et al.</i> [44]	AAAI21	ResNet-101	I, SA	68.2	68.5
Yao <i>et al.</i> [76]	CVPR21	ResNet-101	I, SA	68.3	68.5
AuxSegNet [73]	ICCV21	ResNet38	I, SA	69.0	68.6
SPML [33]	ICLR21	ResNet-101	I, SA	69.5	71.6
EDAM [63]	CVPR21	ResNet-101	I, SA	70.9	70.6
DRS [34]	AAAI21	ResNet-101	I, SA	71.2	71.4
ICD [14]	CVPR20	ResNet-101	I	64.1	64.3
IRN [1]	CVPR19	ResNet50	I	63.5	64.8
SSDD [60]	ICCV19	ResNet-38	I	64.9	65.5
SEAM [71]	CVPR20	ResNet-38	I	64.5	65.7
Chang <i>et al.</i> [8]	CVPR20	ResNet-101	I	66.1	65.9
RRM [77]	AAAI20	ResNet-101	I	66.3	66.5
BES [9]	ECCV20	ResNet-101	I	65.7	66.6
Ru <i>et al.</i> [59]	IJCAI21	ResNet101	I	67.2	67.3
CONTA [78]	NIPS20	ResNet-101	I	66.1	66.7
ECS-Net [63]	ICCV21	ResNet38	I	66.6	67.6
CPN [79]	ICCV21	ResNet38	I	67.8	68.5
AdvCAM [40]	CVPR21	ResNet-101	I	68.1	68.0
PMM [45]	ICCV21	ResNet-38	I	68.5	69.0
Ours	-	ResNet-101	I	68.5	68.4 ³
PMM [45]	ICCV21	Res2Net101	I	70.0	70.5
Ours	-	Res2Net101	I	71.0	71.0 ⁴

common practice [40, 77], we train our model on 10582 images where the extra images and annotations are from [21]. We report the evaluation results on 1449 validation images and 1456 test images. We adopt mean intersection-over-union (mIoU) as the evaluation metric.

Implementation Details. For implementing our approach, we use the single-teacher distillation model [77] as our baseline. The specific settings can be referred to the supplementary material.

For a training image, we resize it with a random ratio from (0.7, 1.3), and then apply a random flip. Finally, it is normalized and cropped to size 321×321 . For the Pulse Width Modulation, we set $T = 150$ and $\tau = 5$. To generate reliable pseudo labels, the scale ratio of multi-scale CAM is set to {0.5, 1, 1.5, 2}. During testing, Dense CRF is used as post-processing. We use the SGD optimizer [7] with momentum 0.9 and weight decay $1e-5$. The learning rate is

0.0007. We train the network for 8 epochs with a batch size of 4. We set $\sigma_D = 15$ and $\sigma_I = 100$ as [77].

We use two different methods as the the final segmentation model. Firstly, following [9, 40, 77, 78], we utilize a PyTorch implementation of the DeepLab-v2 [11] with ResNet-101 [22] backbone⁵. Secondly, following [45] we use PSPnet [83] with Res2Net101 [17] backbone as another segmentation model. We set the momentum and weight decay of the SGD optimizer as 0.9 and $5e-4$, respectively. The initial learning rate is 0.0025 and is decreased using polynomial decay with a power of 0.9. We train the segmentation network for 20000 iterations with batch size 10. The experiments are implemented by Pytorch [54] on an NVIDIA GTX 1080Ti GPU.

4.1. Comparison with Stat-of-the-art Methods

Pascal VOC 2012. In Table 1, we compare our proposed method with state-of-the-art methods that are learned with various levels of annotation, including fully supervised masks (F), bounding boxes (B), scribbles (S), or image class labels (I), with and without extra data. We report the performance of the final segmentation model. According to the experimental results, our method obtains mIoU of 68.5% and 68.4% on validation and test set. Our method achieves 2.2% and 1.9% performance gains than our baseline model RRM on validation and test set, respectively. Compared to other start-of-the-art methods without using saliency maps, when the segmentation model is DeepLab-v2 with ResNet-101 backbone, our methods achieve the same results as PMM on the validation set and slightly underperforms PMM on the test set. When the PSPnet with Res2Net101 backbone is used as the segmentation model, our ASDT outperforms PMM on both validation and test set. In the supplementary material, we provide the per-class comparison with other methods. Some visualization examples of the proposed approach are shown in Fig. 5, we provide six successful examples and three failed examples. In particular, we can observe from three failed examples that it is still difficult for our method to distinguish group objects overlapping with each other.

COCO-Stuff 10k. Apart from PASCAL VOC 2012, we also provide results on COCO-Stuff 10K [47] dataset. Following EDAM [72], we selected 9000 images that belong to the 20 categories of PASCAL VOC for training and set pixels of other categories as background. The segmentation model is DeepLab-v2 with ResNet-101 backbone. As shown in Table 9, our ASDT brings 0.6% performance gains over baseline RRM. Moreover, our ASDT outperforms EDAM, which uses saliency maps in post-processing. Those results demonstrate the proposed ASDT can perform well in more complex scenarios.

⁵<https://github.com/kazuto1011/deeplab-pytorch>



Figure 5. Examples of semantic masks predicted by our ASDT. We provide six successful examples (left) and three failed examples (right).

Table 2. Experimental results of ResNet101 backbone on COCO-Stuff 10K. The supervision information (Sup.) includes: F (full pixel-level supervision), I (image-level supervision), SA (saliency maps). [†] denotes the results from EDAM [72]

Method	Sup.	test
Deeplab-v2 [11] [†]	F	55.9
EDAM [72] [†]	I, SA	51.4
RRM [77]	I	51.4
Ours	I	52.0

4.2. Experiments with Extra Data

Here we also follow existing works [43, 62, 72] to evaluate the weakly supervised learning performance of the proposed approach by using extra weakly labeled training data. Specifically, the experiments are carried out by using the additional single-label images from the Caltech-256 dataset [19], where around 4k images are selected to align with the object categories presented in PASCAL VOC 2012. The experimental comparison results are reported in Table 3, we can observe our ASDT outperforms all other methods, even some of them use extra saliency maps. Note that MCIS [62] uses 20k extra images from Caltech-256 and ImageNet.

4.3. Ablation Study

In Table 4, we first compare different self-distillation strategies on the validation set of the PASCAL VOC 2012 benchmark. We report the mIoU of the seg-teacher, student, and the final combined prediction for each model. The concrete settings are described as follows:

- In experiment (1), the model only contains a class-teacher branch and a student branch. The network parameters are trained by using \mathcal{L}_{ce} and \mathcal{L}_d^{ct} .
- In experiment (2), the model only contains a class-teacher branch, a seg-teacher branch, and a student branch, learned by \mathcal{L}_{ce} , \mathcal{L}_d^{ct} , and \mathcal{L}_d^{st} , respectively.

Table 3. Comparison with the state-of-the-art approaches on PASCAL VOC 2012 with extra simple single-label images from Caltech-256 [19]. The supervision information (Sup.) includes: I (image-level supervision), SA (saliency maps).

Method	Sup.	val	test
MCNN [66]	I	-	36.9
MIL-seg [56]	I	42.0	40.6
AttnBN [43]	I, SA	66.1	65.9
MCIS [62]	I, SA	67.1	67.2
EDAM [72]	I, SA	72.0	71.4
Ours	I	72.0	71.9 ⁶

- In experiment (3), the model is similar to the experiment (2). The only difference is that when training the student branch, the supervision signal is obtained by performing CRF on $\max(\mathbf{P}^{ct}, \mathbf{P}^{st})$ instead of \mathbf{B}^{st} .
- In experiment (4), the model performs CRF on $\text{mean}(\mathbf{P}^{ct}, \mathbf{P}^{st})$ to train the student branch, while other settings are kept the same with the experiment (3).

From the reported results, we can observe that using the single-teacher model can already achieve a good segmentation performance. However, it is nontrivial to further introduce dual-teaching architecture to learn the student network branch. In particular, as shown in experiment (2), the student branch only achieves a performance of 30.4% mIoU when it is supervised only by the seg-teacher, which reveals that the performance of a segmentation-oriented branch will be seriously affected by the errors from the supervision signal. In fact, the seg-teacher itself can only get 62.3% mIoU or so, which indicates that it would produce lots of miss-classification and be far from a perfect teacher model, especially at the early phase of the learning procedure. Under this circumstance, the conventional direct distillation strat-

⁶<http://host.robots.ox.ac.uk:8080/anonymous/ICEZ2N.html>

Table 4. Analysis about different distillation strategies on the PASCAL VOC 2012 validation set. The reported results are obtained without the retrain process. Detailed discussion on the comparison of different distillation strategies can be referred to in Sec. 4.3.

Distillation Strategy	\mathbf{P}^{st}	\mathbf{P}^s	$\bar{\mathbf{P}}$
Single class-teacher	-	62.6	-
Single seg-teacher	62.3	30.4	48.5
Naive dual teacher (max)	62.4	40.1	53.2
Naive dual teacher (mean)	62.3	40.0	53.6
Alternative dual teacher	63.8	63.8	64.0

egy cannot learn a good student model. In the experiment (3) and (4), two naive ways are tried to combine the two different teacher network branches: using element-wise mean or element-wise max for generating the fused supervision maps. Although the mIoU of the student increases from 30.4% to 40.1% and 40.0%, respectively, such results are still unsatisfactory. Compared to the above four experiments, in experiment (5), we adopt the newly proposed distillation mechanism which alternatively chooses the two different teacher branches. In this case, the performance of the student branch reaches 63.8%, and the mIoU of the combined prediction improves to 64.0%. To the best of our knowledge, the superiority of our learning mechanism is its capacity in correcting the error supervision of the seg-teacher branch at the early learning phase while integrating diverse supervision signals at the late learning phase.

Next, we further study the influence of computational components used in our framework. As shown in Table 5, we mainly study four components, which are the reliable mask \mathbf{R}^{ct} , the structure loss in Eq.8, the CRF post-processing, and the strategies to fuse the two segmentation branches to obtain the pseudo annotation, including the mean, multiply, and max operation. From the comparison results, we can observe that the reliable mask and structure loss play a critical role in guiding the learning procedure, while the CRF post-processing can also improve the quality of the segmentation results by near 3%. As for the fusion strategy, the mean and max operation perform equally well (the latter is slightly better) but the multiply operation performs worse than the other two strategies.

4.4. Analysis on the Pulse Width Modulation

The proposed alternative distillation mechanism is determined by a pulse width modulation, and the shape of the PW wave is controlled by alternation period width T and alternation proportion τ . In Fig. 6, we analyze how these two hyper-parameters affect the performance of the proposed alternative self-dual teaching model.

Alternation period width T : it determines how many iterations in a single self-dual teaching period. As shown in

Table 5. Ablation study of different components used in our framework on the PASCAL VOC 2012 validation set. The reported results are obtained without the retrain process.

\mathbf{R}^{ct}	\mathcal{L}_{str}	CRF	Mean	Multiply	Max	mIoU
	✓	✓			✓	44.51
✓		✓			✓	51.37
✓	✓				✓	61.33
✓	✓	✓	✓			64.02
✓	✓	✓		✓		62.99
✓	✓	✓			✓	64.03

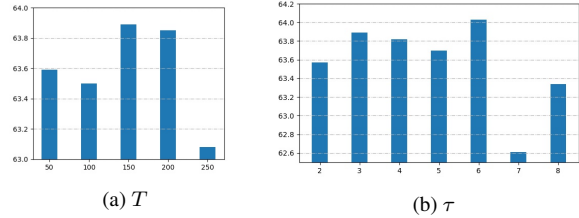


Figure 6. Performance of using different values for T and τ on the PASCAL VOC 2012 validation set. The reported results are obtained without the retrain process.

the upper figure of Fig. 6, we compared five different period widths. From the experimental results, we can observe that different period widths would seriously affect the performance (64.03 for $T = 150$ VS. 63.08 for $T = 250$).

Alternation proportion τ : It determines the proportion of the class-teacher and the seg-teacher within a self-dual teaching period. As shown in the bottom of Fig. 6, varying τ to different values obtains performance with a relative flattening curve, which demonstrates that the proposed self-dual teaching process is less sensitive to the proportion of the class teacher and the seg-teacher.

5. Conclusion

In this paper, we build a unified deep model for generating the pseudo segmentation masks under weak image-level supervision. To enrich knowledge sharing and interaction, we establish a self-dual teaching architecture and propose the novel alternative distillation mechanism, which forms the overall alternative self-dual teaching (ASDT) framework. To avoid getting into the undesired local minimum that may be produced by either teacher, we introduce a PW wave-like selection signal to facilitate the alternative knowledge distillation. Comprehensive experiments demonstrate the effectiveness of the proposed approach.

Limitation. The current approach is relatively time consuming in the learning stage, which would prevent using it in large-scale test scenarios. In the future, we will further improve the learning framework to overcome this limitation.

References

- [1] Jiwoon Ahn, Sunghyun Cho, and Suha Kwak. Weakly supervised learning of instance segmentation with inter-pixel relations. In *CVPR*, pages 2209–2218, 2019. 3, 6
- [2] Jiwoon Ahn and Suha Kwak. Learning pixel-level semantic affinity with image-level supervision for weakly supervised semantic segmentation. In *CVPR*, pages 4981–4990, 2018. 3, 13
- [3] Bogdan Alexe, Thomas Deselaers, and Vittorio Ferrari. Measuring the objectness of image windows. *TPAMI*, 34(11):2189–2202, 2012. 2
- [4] Jimmy Ba and Rich Caruana. Do deep nets really need to be deep? In *NIPS*, pages 2654–2662, 2014. 2, 3
- [5] Amy Bearman, Olga Russakovsky, Vittorio Ferrari, and Li Fei-Fei. What’s the point: Semantic segmentation with point supervision. In *ECCV*, pages 549–565. Springer, 2016. 1, 3
- [6] Ali Borji, Ming-Ming Cheng, Huaizu Jiang, and Jia Li. Salient object detection: A benchmark. *TIP*, 24(12):5706–5722, 2015. 3
- [7] Léon Bottou. Large-scale machine learning with stochastic gradient descent. In *COMPSTAT*, pages 177–186. Springer, 2010. 6
- [8] Yu-Ting Chang, Qiaosong Wang, Wei-Chih Hung, Robinson Piramuthu, Yi-Hsuan Tsai, and Ming-Hsuan Yang. Weakly-supervised semantic segmentation via sub-category exploration. In *CVPR*, pages 8991–9000, 2020. 1, 3, 6, 13
- [9] Liyi Chen, Weiwei Wu, Chenchen Fu, Xiao Han, and Yuntao Zhang. Weakly supervised semantic segmentation with boundary exploration. In *ECCV*, pages 347–362. Springer, 2020. 2, 3, 6, 13
- [10] Liang-Chieh Chen, George Papandreou, Iasonas Kokkinos, Kevin Murphy, and Alan L. Yuille. Semantic image segmentation with deep convolutional nets and fully connected crfs. In *ICLR*, 2015. 3, 6
- [11] Liang-Chieh Chen, George Papandreou, Iasonas Kokkinos, Kevin Murphy, and Alan L Yuille. Deeplab: Semantic image segmentation with deep convolutional nets, atrous convolution, and fully connected crfs. *TPAMI*, 40(4):834–848, 2017. 3, 6, 7
- [12] Jifeng Dai, Kaiming He, and Jian Sun. Boxsup: Exploiting bounding boxes to supervise convolutional networks for semantic segmentation. In *ICCV*, pages 1635–1643, 2015. 1, 3
- [13] Mark Everingham, Luc Van Gool, Christopher KI Williams, John Winn, and Andrew Zisserman. The pascal visual object classes (voc) challenge. *IJCV*, 88(2):303–338, 2010. 5
- [14] Junsong Fan, Zhaoxiang Zhang, Chunfeng Song, and Tieniu Tan. Learning integral objects with intra-class discriminator for weakly-supervised semantic segmentation. In *CVPR*, pages 4283–4292, 2020. 2, 3, 6
- [15] Junsong Fan, Zhaoxiang Zhang, and Tieniu Tan. Employing multi-estimations for weakly-supervised semantic segmentation. In *ECCV*. Springer, 2020. 1, 3, 6
- [16] Ruochen Fan, Qibin Hou, Ming-Ming Cheng, Gang Yu, Ralph R Martin, and Shi-Min Hu. Associating inter-image salient instances for weakly supervised semantic segmentation. In *ECCV*, pages 367–383, 2018. 3
- [17] Shanghua Gao, Ming-Ming Cheng, Kai Zhao, Xin-Yu Zhang, Ming-Hsuan Yang, and Philip HS Torr. Res2net: A new multi-scale backbone architecture. *TPAMI*, 2019. 6, 12
- [18] Jianping Gou, Baosheng Yu, Stephen J Maybank, and Dacheng Tao. Knowledge distillation: A survey. *IJCV*, pages 1–31, 2021. 2, 3
- [19] Gregory Griffin, Alex Holub, and Pietro Perona. Caltech-256 object category dataset. 2007. 7, 12, 13
- [20] Junwei Han, Dingwen Zhang, Gong Cheng, Nian Liu, and Dong Xu. Advanced deep-learning techniques for salient and category-specific object detection: a survey. *SPM*, 35(1):84–100, 2018. 2
- [21] Bharath Hariharan, Pablo Arbeláez, Lubomir Bourdev, Subhransu Maji, and Jitendra Malik. Semantic contours from inverse detectors. In *ICCV*, pages 991–998. IEEE, 2011. 6
- [22] Kaiming He, Xiangyu Zhang, Shaoqing Ren, and Jian Sun. Deep residual learning for image recognition. In *CVPR*, pages 770–778. IEEE, 2016. 6
- [23] Geoffrey Hinton, Oriol Vinyals, and Jeff Dean. Distilling the knowledge in a neural network. *arXiv*, 2015. 2, 3
- [24] Seunghoon Hong, Donghun Yeo, Suha Kwak, Honglak Lee, and Bohyung Han. Weakly supervised semantic segmentation using web-crawled videos. In *CVPR*, pages 7322–7330, 2017. 3
- [25] Qibin Hou, PengTao Jiang, Yunchao Wei, and Ming-Ming Cheng. Self-erasing network for integral object attention. *NIPS*, 31:549–559, 2018. 3
- [26] Qibin Hou, Daniela Massiceti, Puneet Kumar Dokania, Yunchao Wei, Ming-Ming Cheng, and Philip HS Torr. Bottom-up top-down cues for weakly-supervised semantic segmentation. In *EMMCVPR*, pages 263–277. Springer, 2017. 3
- [27] Zilong Huang, Xinggang Wang, Jiasi Wang, Wenyu Liu, and Jingdong Wang. Weakly-supervised semantic segmentation network with deep seeded region growing. In *CVPR*, pages 7014–7023, 2018. 1, 3
- [28] Zeyi Huang, Yang Zou, BVK Kumar, and Dong Huang. Comprehensive attention self-distillation for weakly-supervised object detection. *NIPS*, 33, 2020. 3
- [29] Guangda Ji and Zhanxing Zhu. Knowledge distillation in wide neural networks: Risk bound, data efficiency and imperfect teacher. 2020. 5
- [30] Peng-Tao Jiang, Qibin Hou, Yang Cao, Ming-Ming Cheng, Yunchao Wei, and Hong-Kai Xiong. Integral object mining via online attention accumulation. In *ICCV*, pages 2070–2079, 2019. 2
- [31] Bin Jin, Maria V Ortiz Segovia, and Sabine Susstrunk. Webly supervised semantic segmentation. In *CVPR*, pages 3626–3635, 2017. 3
- [32] Seong Joon Oh, Rodrigo Benenson, Anna Khoreva, Zeynep Akata, Mario Fritz, and Bernt Schiele. Exploiting saliency for object segmentation from image level labels. In *CVPR*, pages 4410–4419, 2017. 3
- [33] Tsung-Wei Ke, Jyh-Jing Hwang, and Stella X Yu. Universal weakly supervised segmentation by pixel-to-segment contrastive learning. *arXiv*, 2021. 3, 6
- [34] Beomyoung Kim, Sangeun Han Kim, et al. Discriminative region suppression for weakly-supervised semantic segmentation. *arXiv*, 2021. 2, 3, 6

- [35] Dahun Kim, Donghyeon Cho, Donggeun Yoo, and In So Kweon. Two-phase learning for weakly supervised object localization. In *ICCV*, pages 3534–3543, 2017. 3, 13
- [36] Alexander Kolesnikov and Christoph H Lampert. Seed, expand and constrain: Three principles for weakly-supervised image segmentation. In *ECCV*, pages 695–711. Springer, 2016. 3, 13
- [37] Hankook Lee, Sung Ju Hwang, and Jinwoo Shin. Rethinking data augmentation: Self-supervision and self-distillation. 2019. 3
- [38] Jungbeom Lee, Eunji Kim, Sungmin Lee, Jangho Lee, and Sungroh Yoon. Ficklenet: Weakly and semi-supervised semantic image segmentation using stochastic inference. In *CVPR*, pages 5267–5276, 2019. 3
- [39] Jungbeom Lee, Eunji Kim, Sungmin Lee, Jangho Lee, and Sungroh Yoon. Frame-to-frame aggregation of active regions in web videos for weakly supervised semantic segmentation. In *ICCV*, pages 6808–6818, 2019. 3, 6
- [40] Jungbeom Lee, Eunji Kim, and Sungroh Yoon. Anti-adversarially manipulated attributions for weakly and semi-supervised semantic segmentation. *arXiv*, 2021. 1, 3, 6
- [41] Jungbeom Lee, Jihun Yi, Chaehun Shin, and Sungroh Yoon. Bbam: Bounding box attribution map for weakly supervised semantic and instance segmentation. *arXiv*, 2021. 3, 6
- [42] Kunpeng Li, Ziyang Wu, Kuan-Chuan Peng, Jan Ernst, and Yun Fu. Tell me where to look: Guided attention inference network. In *CVPR*, pages 9215–9223, 2018. 3
- [43] Kunpeng Li, Yulun Zhang, Kai Li, Yuanyuan Li, and Yun Fu. Attention bridging network for knowledge transfer. In *ICCV*, pages 5198–5207, 2019. 7
- [44] Xueyi Li, Tianfei Zhou, Jianwu Li, Yi Zhou, and Zhaoxiang Zhang. Group-wise semantic mining for weakly supervised semantic segmentation. *arXiv*, 2020. 3, 6
- [45] Yi Li, Zhanghui Kuang, Liyang Liu, Yimin Chen, and Wayne Zhang. Pseudo-mask matters in weakly-supervised semantic segmentation. In *ICCV*, pages 6964–6973, 2021. 3, 6
- [46] Di Lin, Jifeng Dai, Jiaya Jia, Kaiming He, and Jian Sun. Scribblesup: Scribble-supervised convolutional networks for semantic segmentation. In *CVPR*, pages 3159–3167, 2016. 1, 3
- [47] Tsung-Yi Lin, Michael Maire, Serge Belongie, James Hays, Pietro Perona, Deva Ramanan, Piotr Dollár, and C Lawrence Zitnick. Microsoft coco: Common objects in context. In *ECCV*, pages 740–755. Springer, 2014. 5, 6
- [48] Yun Liu, Yu-Huan Wu, Pei-Song Wen, Yu-Jun Shi, Yu Qiu, and Ming-Ming Cheng. Leveraging instance-, image- and dataset-level information for weakly supervised instance segmentation. *TPAMI*, 2020. 3, 6
- [49] Jonathan Long, Evan Shelhamer, and Trevor Darrell. Fully convolutional networks for semantic segmentation. In *CVPR*, pages 3431–3440, 2015. 1
- [50] R Austin McEver and BS Manjunath. Pcams: Weakly supervised semantic segmentation using point supervision. *arXiv*, 2020. 1, 3
- [51] Youngmin Oh, Beomjun Kim, and Bumsu Ham. Background-aware pooling and noise-aware loss for weakly-supervised semantic segmentation. *arXiv*, 2021. 3
- [52] George Papandreou, Liang-Chieh Chen, Kevin P Murphy, and Alan L Yuille. Weakly-and semi-supervised learning of a deep convolutional network for semantic image segmentation. In *ICCV*, pages 1742–1750, 2015. 1, 3, 6, 13
- [53] Nikolaos Passalis and Anastasios Tefas. Learning deep representations with probabilistic knowledge transfer. In *ECCV*, pages 268–284, 2018. 3
- [54] Adam Paszke, Sam Gross, Soumith Chintala, Gregory Chanan, Edward Yang, Zachary DeVito, Zeming Lin, Alban Desmaison, Luca Antiga, and Adam Lerer. Automatic differentiation in pytorch. In *NIPS*, 2017. 6
- [55] Mary Phuong and Christoph H Lampert. Distillation-based training for multi-exit architectures. In *ICCV*, pages 1355–1364, 2019. 3
- [56] Pedro O Pinheiro and Ronan Collobert. From image-level to pixel-level labeling with convolutional networks. In *CVPR*, pages 1713–1721, 2015. 7, 13
- [57] Xiaojuan Qi, Zhengzhe Liu, Jianping Shi, Hengshuang Zhao, and Jiaya Jia. Augmented feedback in semantic segmentation under image level supervision. In *ECCV*, pages 90–105. Springer, 2016. 3
- [58] Adriana Romero, Nicolas Ballas, Samira Ebrahimi Kahou, Antoine Chassang, Carlo Gatta, and Yoshua Bengio. Fitnets: Hints for thin deep nets. In *ICLR*, 2015. 3
- [59] Lixiang Ru, Bo Du, and Chen Wu. Learning visual words for weakly-supervised semantic segmentation. In *IJCAI*, 2021. 6
- [60] Wataru Shimoda and Keiji Yanai. Self-supervised difference detection for weakly-supervised semantic segmentation. In *CVPR*, pages 5208–5217, 2019. 3, 6, 13
- [61] Chunfeng Song, Yan Huang, Wanli Ouyang, and Liang Wang. Box-driven class-wise region masking and filling rate guided loss for weakly supervised semantic segmentation. In *CVPR*, pages 3136–3145, 2019. 3
- [62] Guolei Sun, Wenguan Wang, Jifeng Dai, and Luc Van Gool. Mining cross-image semantics for weakly supervised semantic segmentation. In *ECCV*, pages 347–365. Springer, 2020. 1, 3, 6, 7
- [63] Kunyang Sun, Haoqing Shi, Zhengming Zhang, and Yongming Huang. Ecs-net: Improving weakly supervised semantic segmentation by using connections between class activation maps. In *CVPR*, pages 7283–7292, 2021. 6
- [64] Meng Tang, Abdelaziz Djelouah, Federico Perazzi, Yuri Boykov, and Christopher Schroers. Normalized cut loss for weakly-supervised cnn segmentation. In *CVPR*, pages 1818–1827, 2018. 1, 3
- [65] Meng Tang, Federico Perazzi, Abdelaziz Djelouah, Ismail Ben Ayed, Christopher Schroers, and Yuri Boykov. On regularized losses for weakly-supervised cnn segmentation. In *ECCV*, pages 507–522, 2018. 1, 3, 5, 6
- [66] Pavel Tokmakov, Karteek Alahari, and Cordelia Schmid. Weakly-supervised semantic segmentation using motion cues. In *ECCV*, pages 388–404. Springer, 2016. 7
- [67] Frederick Tung and Greg Mori. Similarity-preserving knowledge distillation. In *ICCV*, pages 1365–1374, 2019. 3
- [68] Bin Wang, Guojun Qi, Sheng Tang, Tianzhu Zhang, Yunchao Wei, Linghui Li, and Yongdong Zhang. Boundary perception guidance: A scribble-supervised semantic segmentation approach. In *IJCAI*, pages 3663–3669, 2019. 1, 3, 6

- [69] Wenguan Wang, Tianfei Zhou, Fisher Yu, Jifeng Dai, Ender Konukoglu, and Luc Van Gool. Exploring cross-image pixel contrast for semantic segmentation. *arXiv*, 2021. 1
- [70] Xiang Wang, Sifei Liu, Huimin Ma, and Ming-Hsuan Yang. Weakly-supervised semantic segmentation by iterative affinity learning. *IJCV*, 128(6):1736–1749, 2020. 3
- [71] Yude Wang, Jie Zhang, Meina Kan, Shiguang Shan, and Xilin Chen. Self-supervised equivariant attention mechanism for weakly supervised semantic segmentation. In *CVPR*, pages 12275–12284, 2020. 1, 3, 6, 13
- [72] Tong Wu, Junshi Huang, Guangyu Gao, Xiaoming Wei, Xiaolin Wei, Xuan Luo, and Chi Harold Liu. Embedded discriminative attention mechanism for weakly supervised semantic segmentation. In *CVPR*, pages 16765–16774, 2021. 6, 7
- [73] Lian Xu, Wanli Ouyang, Mohammed Bennamoun, Farid Boussaid, Ferdous Sohel, and Dan Xu. Leveraging auxiliary tasks with affinity learning for weakly supervised semantic segmentation. In *ICCV*, pages 6984–6993, 2021. 3, 6
- [74] Chenglin Yang, Lingxi Xie, Chi Su, and Alan L Yuille. Snapshot distillation: Teacher-student optimization in one generation. In *CVPR*, pages 2859–2868, 2019. 3
- [75] Peng Yang, Guowei Yang, Xun Gong, Pingping Wu, Xu Han, Jiasong Wu, and Caisen Chen. Instance segmentation network with self-distillation for scene text detection. *IEEE Access*, 8:45825–45836, 2020. 3
- [76] Yazhou Yao, Tao Chen, Guosen Xie, Chuanyi Zhang, Fumin Shen, Qi Wu, Zhenmin Tang, and Jian Zhang. Non-salient region object mining for weakly supervised semantic segmentation. In *CVPR*, 2021. 2, 6
- [77] Bingfeng Zhang, Jimin Xiao, Yunchao Wei, Mingjie Sun, and Kaizhu Huang. Reliability does matter: An end-to-end weakly supervised semantic segmentation approach. In *AAAI*, volume 34, pages 12765–12772, 2020. 2, 3, 4, 6, 7, 12, 13
- [78] Dong Zhang, Hanwang Zhang, Jinhui Tang, Xian-Sheng Hua, and Qianru Sun. Causal intervention for weakly-supervised semantic segmentation. *NIPS*, 33, 2020. 1, 3, 6
- [79] Fei Zhang, Chaochen Gu, Chenyue Zhang, and Yuchao Dai. Complementary patch for weakly supervised semantic segmentation. In *ICCV*, pages 7242–7251, 2021. 3, 6
- [80] Linfeng Zhang, Jiebo Song, Anni Gao, Jingwei Chen, Chenglong Bao, and Kaisheng Ma. Be your own teacher: Improve the performance of convolutional neural networks via self distillation. In *ICCV*, pages 3713–3722, 2019. 3
- [81] Tianyi Zhang, Guosheng Lin, Weide Liu, Jianfei Cai, and Alex Kot. Splitting vs. merging: Mining object regions with discrepancy and intersection loss for weakly supervised semantic segmentation. In *ECCV*, 2020. 2, 3
- [82] Zhilu Zhang and Mert R Sabuncu. Self-distillation as instance-specific label smoothing. In *NIPS*, 2020. 2
- [83] Hengshuang Zhao, Jianping Shi, Xiaojuan Qi, Xiaogang Wang, and Jiaya Jia. Pyramid scene parsing network. In *CVPR*, pages 2881–2890, 2017. 6, 12
- [84] Bolei Zhou, Aditya Khosla, Agata Lapedriza, Aude Oliva, and Antonio Torralba. Learning deep features for discriminative localization. In *CVPR*, pages 2921–2929, 2016. 1, 3, 4

In the appendix, we first provide a per-class performance comparison with several previous works, then we provide three detailed visualization figures and the corresponding analyses.

A. Per-class Performance

In Table 6 and 7, we provide the concrete performance on the VOC 2012 *val* and *test* set, respectively. We report the results obtained from two segmentation models, *i.e.* the Deeplab models with ResNet101 backbone and PSPnet [83] with Res2Net101 [17] backbone. Our ASDT can obtain substantial performance improvement compared to other methods. In addition, in Table 8 we provide the per-class performance on the PASCAL VOC 2012 with extra data from Caltech-256 dataset [19] dataset. The segmentation model is PSPnet [83] with Res2Net101 [17] backbone. Finally, we provide the per-class performance on the COCO Stuff 10K dataset in Table 9. The segmentation model is Deeplab models with ResNet101 backbone.

B. More Visualizations

In this section, we provide three detailed visualization figures to help better understand the proposed methods. Firstly, we visualized the predicted masks of every component in our method. Moreover, we provide a qualitative comparison between the proposed ASDT method and baseline RRM. Finally, we give an example to illustrate the results of self-dual teaching architecture obtained in different training epochs.

Visualization of every step in ASDT. The complete ASDT consists of the self-dual teaching network and a PSPnet model [83]. It mainly contains three branches, *i.e.* a class-teacher, a seg-teacher, and a student. In Fig. 7, We visualized some qualitative results of the predicted masks for every component in ASDT, *i.e.* predictions from class-teacher, seg-teacher, student, combined predictions of the seg-teacher and student, and the final predictions of the PSPnet model. We provide six success cases and three failure cases. For the first failure case, our method produces the wrong classification results. For the second failure case, our method doesn't produce the fine label. For the third failure case, our method produces the wrong segmentation results between foreground category and background category.

Qualitative comparison to the baseline. Fig. 8 shows the qualitative segmentation mask comparisons between our proposed ASDT and baseline RRM [77]. We can observe that ASDT can make more accurate predictions on object boundary than RRM. The main reason is that we tactfully introduce a novel supervision information, *i.e.* predictions from the seg-teacher, which contains more complex foreground and background annotations so that the network can better distinguish the boundary position.

Table 6. Comparison of per-class semantic segmentation performance on the PASCAL VOC 2012 *val* set.

	bkg	aero	bike	bird	boat	bottle	bus	car	cat	chair	cow	table	dog	horse	motor	person	plant	sheep	sofa	train	tv	mIOU
EM-Adapt [52]	67.2	29.2	17.6	28.6	22.2	29.6	47.0	44.0	44.2	14.6	35.1	24.9	41.0	34.8	41.6	32.1	24.8	37.4	24.0	38.1	31.6	33.8
MIL+seg [56]	79.6	50.2	21.6	40.9	34.9	40.5	45.9	51.5	60.6	12.6	51.2	11.6	56.8	52.9	44.8	42.7	31.2	55.4	21.5	38.8	36.9	42.0
SEC [36]	82.4	62.9	26.4	61.6	27.6	38.1	66.6	62.7	75.2	22.1	53.5	28.3	65.8	57.8	62.3	52.5	32.5	62.6	32.1	45.4	45.3	50.7
TPL [35]	82.8	62.2	23.1	65.8	21.1	43.1	71.1	66.2	76.1	21.3	59.6	35.1	70.2	58.8	62.3	66.1	35.8	69.9	33.4	45.9	45.6	53.1
PSA [2]	88.2	68.2	30.6	81.1	49.6	61.0	77.8	66.1	75.1	29.0	66.0	40.2	80.4	62.0	70.4	73.7	42.5	70.7	42.6	68.1	51.6	61.7
SEAM [71]	88.8	68.5	33.3	85.7	40.4	67.3	78.9	76.3	81.9	29.1	75.5	48.1	79.9	73.8	71.4	75.2	48.9	79.8	40.9	58.2	53.0	64.5
SSDD [60]	89.0	62.5	28.9	83.7	52.9	59.5	77.6	73.7	87.0	34.0	83.7	47.6	84.1	77.0	73.9	69.6	29.8	84.0	43.2	68.0	53.4	64.9
BES [9]	88.9	74.1	29.8	81.3	53.3	69.9	89.4	79.8	84.2	27.9	76.9	46.6	78.8	75.9	72.2	70.4	50.8	79.4	39.9	65.3	44.8	65.7
Chang <i>et al.</i> [8]	88.8	51.6	30.3	82.9	53.0	75.8	88.6	74.8	86.6	32.4	79.9	53.8	82.3	78.5	70.4	71.2	40.2	78.3	42.9	66.8	58.8	66.1
Ours (ResNet101)	90.0	77.7	31.9	84.9	44.4	74.9	84.9	78.1	87.3	33.6	84.4	52.5	81.8	80.0	71.6	76.0	52.9	84.3	45.4	54.5	67.4	68.5
Ours (Res2Net101)	91.0	81.0	33.4	88.2	50.7	73.5	84.3	80.6	89.8	36.2	88.7	55.6	85.9	83.5	73.2	76.4	60.0	86.4	47.2	57.0	67.5	71.0

Table 7. Comparison of per-class semantic segmentation performance on the PASCAL VOC 2012 *test* set.

	bkg	aero	bike	bird	boat	bottle	bus	car	cat	chair	cow	table	dog	horse	motor	person	plant	sheep	sofa	train	tv	mIOU
EM-Adapt [52]	76.3	37.1	21.9	41.6	26.1	38.5	50.8	44.9	48.9	16.7	40.8	29.4	47.1	45.8	54.8	28.2	30.0	44.0	29.2	34.3	46.0	39.6
MIL+seg [56]	78.7	48.0	21.2	31.1	28.4	35.1	51.4	55.5	52.8	7.8	56.2	19.9	53.8	50.3	40.0	38.6	27.8	51.8	24.7	33.3	46.3	40.6
SEC [36]	83.5	56.4	28.5	64.1	23.6	46.5	70.6	58.5	71.3	23.2	54.0	28.0	68.1	62.1	70.0	55.0	38.4	58.0	39.9	38.4	48.3	51.7
TPL [35]	83.4	62.2	26.4	71.8	18.2	49.5	66.5	63.8	73.4	19.0	56.6	35.7	69.3	61.3	71.7	69.2	39.1	66.3	44.8	35.9	45.5	53.8
PSA [2]	89.1	70.6	31.6	77.2	42.2	68.9	79.1	66.5	74.9	29.6	68.7	56.1	82.1	64.8	78.6	73.5	50.8	70.7	47.7	63.9	51.1	63.7
SSDD [60]	89.5	71.8	31.4	79.3	47.3	64.2	79.9	74.6	84.9	30.8	73.5	58.2	82.7	73.4	76.4	69.9	37.4	80.5	54.5	65.7	50.3	65.5
BES [9]	89.5	71.8	31.4	79.3	47.3	64.2	79.9	74.6	84.9	30.8	73.5	58.2	82.7	73.4	76.4	69.9	37.4	80.5	54.5	65.7	50.3	65.5
Ours (ResNet101)	90.0	81.1	31.5	85.1	41.0	67.6	85.9	78.9	89.2	33.1	78.2	58.1	82.1	81.3	77.0	74.1	54.0	83.0	57.2	44.8	62.6	68.4
Ours (Res2Net101)	91.2	82.3	35.2	91.2	47.9	69.6	83.3	82.2	88.7	33.2	81.9	62.0	82.3	84.6	80.9	75.6	66.4	82.6	58.6	46.5	64.4	71.0

Table 8. Comparison of per-class semantic segmentation performance on the PASCAL VOC 2012 with extra data from Caltech-256 dataset [19]. Backbone is Res2Net101.

	bkg	aero	bike	bird	boat	bottle	bus	car	cat	chair	cow	table	dog	horse	motor	person	plant	sheep	sofa	train	tv	mIOU
val	91.5	81.8	35.0	90.0	55.4	75.7	96.6	83.7	91.1	36.7	89.2	43.9	88.4	85.2	76.7	77.9	56.4	88.6	48.9	57.6	71.0	72.0
test	91.6	84.5	35.3	92.4	53.6	70.1	85.3	83.9	91.1	33.7	83.3	53.6	84.5	84.9	81.2	77.2	66.9	85.0	58.7	47.7	66.1	71.9

Table 9. Comparison of per-class semantic segmentation performance on the COCO Stuff 10K *test* set with ResNet101 backbone.

	bkg	aero	bike	bird	boat	bottle	bus	car	cat	chair	cow	table	dog	horse	motor	person	plant	sheep	sofa	train	tv	mIOU
RRM [77]	86.88	60.77	33.25	31.22	46.81	25.42	69.84	28.54	76.40	15.09	83.42	34.02	65.11	74.49	65.29	73.24	23.13	65.14	39.08	52.35	39.55	51.4
Ours	86.94	62.26	36.76	48.51	47.01	25.35	73.11	28.59	78.51	16.13	77.43	23.92	57.50	68.36	64.43	72.68	25.75	65.20	46.05	48.43	39.91	52.0



Figure 7. Visualization of the predicted masks for each component in ASDT. The last three columns show failure cases.

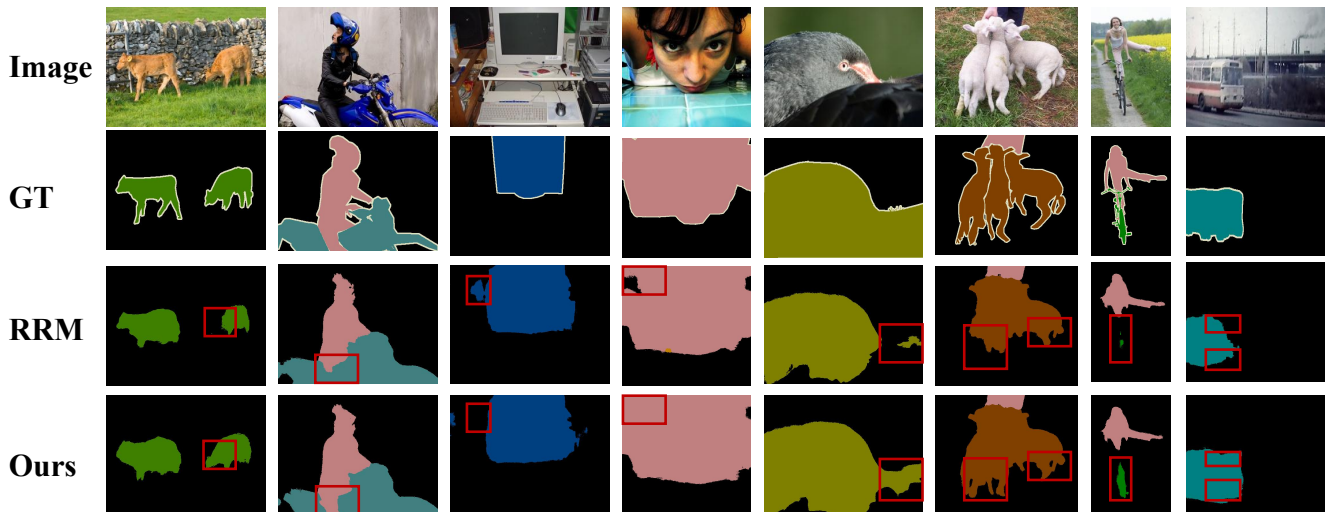


Figure 8. Qualitative comparison between the baseline RRM and our proposed ASDT. Red rectangles highlight the improved regions predicted by ASDT.